Atmospheric Pollution Research 14 (2023) 101694

Contents lists available at ScienceDirect

Atmospheric Pollution Research

journal homepage: www.elsevier.com/locate/apr

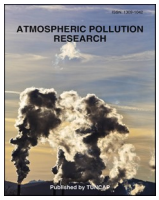

Study of $PM_{2.5}$-bound polycyclic aromatic hydrocarbons and anhydro-sugars in ambient air near two Spanish oil refineries: Covid-19 effects

M.A. Guzmán [a,**], A.J. Fernández [b], C. Boente [a,*], G. Márquez [a], A.M. Sánchez de la Campa [a], E. Lorenzo [c]

[a] Center for Research in Sustainable Chemistry (CIQSO), University of Huelva, 21006, Huelva, Spain
[b] Department of Analytical Chemistry, Faculty of Chemistry University of Sevilla, 41012, Sevilla, Spain
[c] School of Engineering Sciences, State University Santa Elena Peninsula, 240204, La Libertad, Ecuador

ARTICLE INFO

Keywords:
Polycyclic aromatic hydrocarbons
Anhydrosugars
$PM_{2.5}$ fraction
Complex industrial zone
Covid-19
Spain

ABSTRACT

We report the results from a 12 month-long study of the organic compounds associated to $PM_{2.5}$ samples collected around two petroleum refineries (4 samples/month/site) in two complex industrial zones reporting atmospheric pollution issues in the past (Estuary of Huelva and Bay of Algeciras, Spain). Sampling campaign was done from March 2020 when a Covid-19 lockdown was established at Spain to March 2021. Concentrations of fine particulate polycyclic aromatic hydrocarbons (PAHs) and anhydrosugars were separately measured using gas chromatography-mass spectrometry (GC-MS) and ion chromatography-amperometric detection (IC-PAD). The annual average abundances of $PM_{2.5}$-bound benzo[a]pyrene (BaP) are 0.024 and 0.013 $ng{\cdot}m^{-3}$ at La Rábida and Puente Mayorga monitoring stations, while both sites have annual average concentrations of levoglucosan in $PM_{2.5}$ of 14.98 and 9.78 $ng{\cdot}m^{-3}$, respectively. Seasonal variations are observed for concentrations of ΣPAHs and total anhydrosugars in both sampling sites. For PAHs, the highest concentrations averaging c. a. 0.400 (La Rábida) and 0.350 ng m^{-3} (Puente Mayorga) are reported in cold months during December 2020-Febraury 2021 (post-lockdown period), compared to the lowest levels averaging 0.111 and 0.211 $ng{\cdot}m^{-3}$, respectively, in temperate months from mid-March 2020 to early June 2020 (0.284 and 0.321 ng m^{-3} on average annually), coinciding with the confinement and relaxation periods in Spain. Similarly, total anhydrosugars show the highest values of 81.80 $ng{\cdot}m^{-3}$ (La Rábida) and 53.52 $ng{\cdot}m^{-3}$ (Puente Mayorga) in winter and lowest values of 2.71 $ng{\cdot}m^{-3}$ and 3.30 $ng{\cdot}m^{-3}$ into the lockdown period (22.51 and 14.09 $ng{\cdot}m^{-3}$ on average annually). Except phenanthrene, PAHs are present in $PM_{2.5}$ principally as result of motor vehicle exhausts. Levoglucosan, a tracer for biomass burning, peaked in December 2020 and January 2021, during the high residential wood-burning season. In addition, multivariate analysis was used to assess the origin of organic components of $PM_{2.5}$ samples. The two principal components are characterized by the grouping of heavy PAHs associated to vehicular traffic, and anhydrosugars indicating biomass burning emissions, respectively.

1. Introduction

The industrialization may result in fine particulate matter air pollution episodes, particularly when numerous activities are clustered together in complex industrial zones (e.g., Chen et al., 2016; Vega et al., 2021). There is currently few information on the emission of fine particles ($PM_{2.5}$) into the air in complex industrial zones, despite the monitoring of inorganic contaminants (toxic metals) and organic pollutants, such as polycyclic aromatic hydrocarbons (PAHs), and anhydrosugars adhered to $PM_{2.5}$, is certainly an issue of major environmental concern, owing their possible human public health impacts (López-Ayala et al., 2019). Two of the most highly industrialized areas in Spain, which both include a series of facilities (a petroleum refinery, a thermoelectric power plant, and other emitters), are located in Palos de

Peer review under responsibility of Turkish National Committee for Air Pollution Research and Control.
* Corresponding author.
** Corresponding author.
E-mail addresses: marcoantonioguzmanvillanueva@gmail.com (M.A. Guzmán), carlos.boente@dimme.uhu.es (C. Boente).

https://doi.org/10.1016/j.apr.2023.101694
Received 26 October 2022; Received in revised form 23 January 2023; Accepted 13 February 2023
Available online 15 February 2023

la Frontera (Estuary of Huelva) near Huelva city and San Roque (Bay of Algeciras) very close to the Strait of Gibraltar (Fig. 1). Palos de la Frontera and San Roque (including Puente Mayorga) are two small towns located in southwestern Spain, which are susceptible for pollution episodes as a result of atmospheric stability, clear skies and marine aerosols circulation (de la Rosa et al., 2010).

Fine particulate matter ($PM_{2.5}$) air pollution has been associated with several adverse health effects and high levels of mortality and morbidity (Kappos et al., 2004). Apart from fossil fuel combustion, emissions from domestic wood heating and agricultural waste burning are one of the main sources of organic fine and ultrafine particles (Sánchez de la Campa et al., 2018). Organic tracers such as levoglucosan and benzo[a] pyrene (BaP) are measured to estimate biomass burning contributions (Amato et al., 2016; Pérez-Pastor et al., 2020). $PM_{2.5}$-bound PAHs may contribute to acute effects on environment or result in long-term human health risks (Li et al., 2009). Airbone PAHs arise from the incomplete combustion of organic substances and the vaporization of volatile fuels (Alam et al., 2015), being one of the most ubiquitous environmental contaminants known these days (Kim et al., 2012). A group of PAHs (for instance, benzo[a]pyrene) has been classified as probable carcinogenic and mutagenic chemicals and possess cardio-, immune-, hemato-, and neuro-toxicities (Ravindra et al., 2006; IARC Working Group, 2010). The European Commission proposed the most toxic PAH (BaP) as a proxy of ΣPAHs for the development of annual objectives. An annual maximum limit of 1.0 ng m^{-3} for particulate BaP was established by the European Commission. Anhydrosugars, also called monosaccharide anhydrides, are formed by thermal decomposition of hemicellulose and cellulose (Vicente and Alves, 2018). The anhydrosugars levoglucosan (Lev), galactosan (G) and mannosan (M), as tracers for biomass burning (Cheng et al., 2013), were related with altered cellular responses and increases of mutagenic activity (van Den Heuvel et al., 2018). There is no specific regulation on emissions of wood burning tracers in Europe, only some eco-design rules for heating efficiency applied to solid fuel boilers in order to control emissions of organic compounds, among others (European Commission, 2015).

The coronavirus disease 2019 (Covid-19) reached Spain during the first quarter of 2020 and, on 14th March, Spanish Government imposed a lockdown across the country and limiting human mobility to diminish the percentage of population infected by SARS-CoV-2. The confinement period in Spain was from 16th March to 10th May followed by a relaxation period from 11th May to 31st July characterized by a mild reduction in mobility restrictions between regions (Querol et al., 2021). In Bay of Algeciras and Estuary of Huelva, the comparison of the PM_{10} trace element average concentrations in 2020, during the Covid-19 lockdown, and 2013–2016 indicated that road traffic emissions decreased significantly due to mobility restrictions. By contrast, the industrial emissions from these two complex industrial zones located near Huelva and San Roque were maintained during the confinement and relaxation periods (Millán-Martínez et al., 2022).

The aims of this research work were to relate fine particulate organic compounds with their possible sources, with a particular focus on PAHs and anhydrosugars, and to study the interactions between air pollution, meteorology, and Covid-19 lockdown in the areas surrounding the Bay of Algeciras and Estuary of Huelva complex industrial zones in Andalusia. It is envisioned that this research will give valuable information on fine particulate air pollution in complex industrial zones to assess

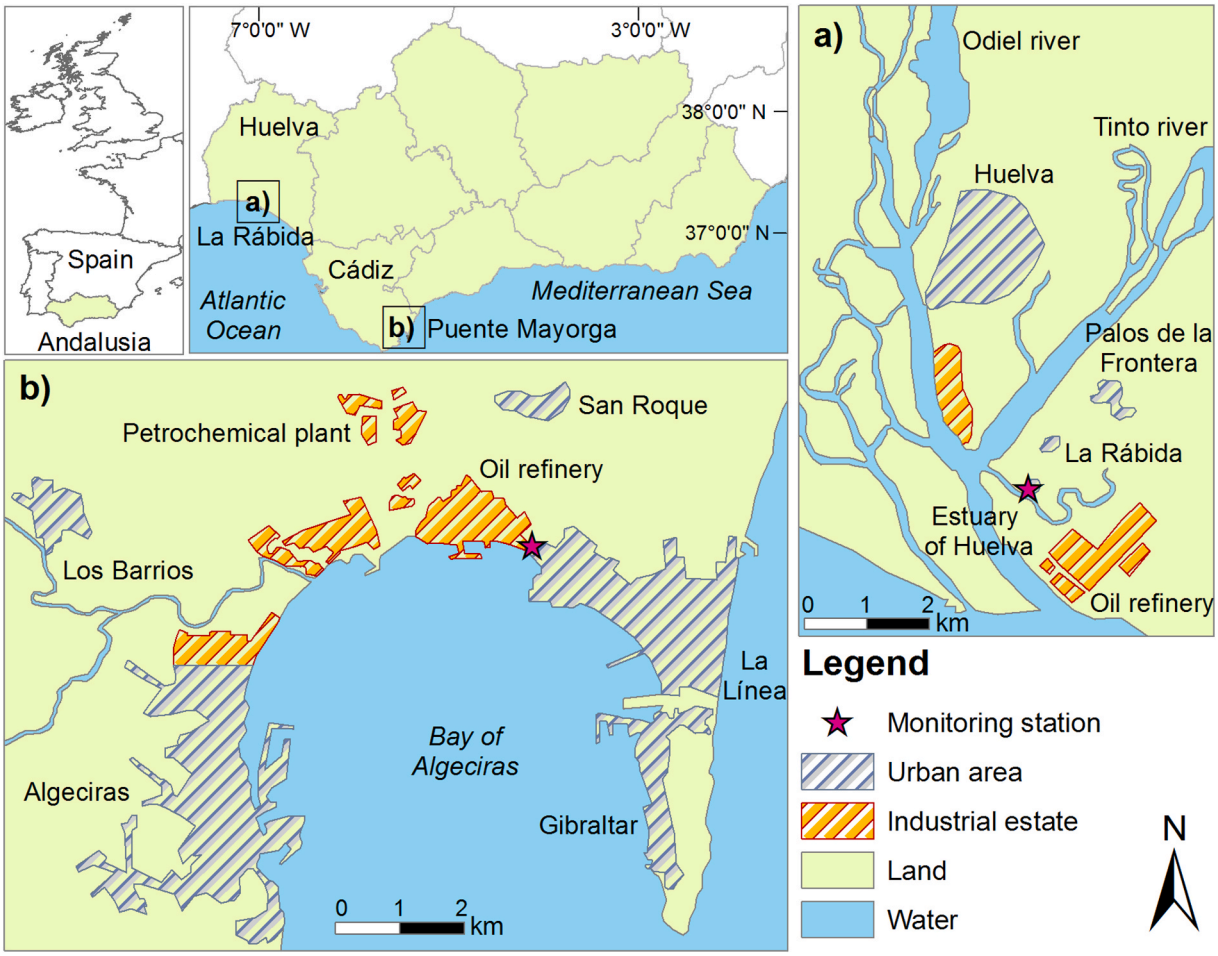

Fig. 1. a) Map showing the location of the Andalusian region in Spain and the study areas which are: a) La Rábida; and b) Puente Mayorga. For each it was included the placement of the monitoring stations as well as the main industrial and urban areas.

further policies for the control of emissions in these two areas.

2. Samples and methods

2.1. Sampling sites and collection

Measurements of $PM_{2.5}$-bound PAHs and monosaccharide anhydrides were conducted at two air quality monitoring stations outside Palos de la Frontera (La Rábida) and inside Puente Mayorga areas, respectively, with the following geographical coordinates: 37°11′ 08″ N, 6°54′03″ W, and 36°11′01″ N, 5°23′48 W (Fig. 1). The location of the sampling sites (about 300 m away the corresponding oil refineries) are shown in Fig. 1. Both stations can be considered as urban/suburban areas with industrial influence and shipping emissions (de la Rosa et al., 2010). Maritime traffic is heavy in the Strait of Gibraltar given its location connecting the Atlantic Ocean to the Mediterranean Sea (Pandolfi et al., 2011). $PM_{2.5}$ fraction was collected from March 2020 to March 2021. Sampling duration was 24 h 47 and 48 p.m.$_{2.5}$ samples, respectively, were taken at Puente Mayorga and La Rábida to characterize the organic aerosol and elucidate sources. Details of the sampling procedure were described in Pindado et al. (2009). The quartz fiber filters (150 mm of diameter) were previously baked out at 400 °C for 6 h for removing organic remnants. After sampling, the filters were equilibrated, weighted, and stored at −20 °C before extraction and analysis. Clean quartz fiber filters were processed as blanks to determine the traces of PAHs and anhydrosugars due to adsorption of components into filter during and after sampling.

$PM_{2.5}$ (particles of aerodynamic diameter ≤2.5 μm), OC, EC, and potassium ion concentrations for daily measured air quality metrics during the sampling period were also taken from the aforementioned sampling stations, which belong to the Andalusia Regional Air Quality Network.

2.2. Sample analyses and quality control

A part of 1/4 of each quartz fiber filter was extracted and derivatized following the methodology of Fontal et al. (2015). Another 1/4 part was extracted for anhydrosacharides. Twelve individual PAHs and other organic compounds were identified and quantified using an Agilent 5977 B-MSD GC-MS (available at the Research Service of the Center for Research in Sustainable Chemistry, University of Huelva). The analytical method used is based on that used by Alier et al. (2013). A mixture of 16 deuterated EPA's priority polyaromatic hydrocarbons (Dr. Ehrenstrofer, PAH-mix 9) was added to each sample as internal standards. Total procedure exhibited recoveries over 90% thus percentages of 100% were assumed. Quantification of PAHs was performed using external standard calibrations. A multipoint calibration curve for each PAH compound was constructed by analyzing aliquots of a standard stock solution (Supelco, EPA 610 PAHs mixture), and high linear correlations ($r > 0.999$) were shown. Detection limits (Table 1) were calculated as three times the standard deviation of results from analysis of six blanks. Concentrations below the respective detection limit and the remaining ones were blank-corrected. Peak identification was undertaken by comparison of mass spectra with literature, comparing of retention times with those of authentic standards, and library data. The fine particulate matter concentrations of 12 PAHs including phenanthrene (Phen), anthracene (Anth), fluoranthene (Flt), pyrene (Pyr), benzo[a]anthracene (BaA), benzo[b]fluoranthene (BbF), benzo[k]fluoranthene (BkF), chrysene (Chry), benzo[a]pyrene (BaP), benzo[g,h,i]perylene (BghiP), indeno[1,2,3-c,d]pyrene (Ind), and dibenzo[a,h]anthracene (DahA) were quantified in $PM_{2.5}$ samples. Naphthalene, acenaphthylene, fluorene, and acenaphthene are not reported here due to analytical artifacts (Kim et al., 2012) and low recoveries (Choi et al., 2007).

Anhydrosugars are analysed by ion chromatography (IC) with pulsed amperometric detection (PAD). Individual monosaccharides levoglucosan (1,6–anhydro-β-D-glucopyranose), mannosan (1,6–anhydro-β-D-mannopyranose) and galactosan (1,6–anhydro-β-D-galactopyranose) were quantified using an Ion Chromatography system from Metröhm (Herisau, Switzerland), equipped with a 940 Professional IC Vario 1 Chromatograph, and a MetroSep Carb 2/150 × 4.0 mm column fixed at 15 °C (polystyrene/divinylbenzene copolymer with quaternary ammonium groups, 5 μm of particle size), specific for separation of carbohydrates, mobil phase of NaOH:NaAcO 300:1 mM at a follow of 0.50 mL min^{-1}. The three anhydrosugars were analysed by pulsed amperometric detection (PAD) after injection with a peek sample loop of 250 μL. For this a 945 Amperometric Detector IC Vario from Metröhm was employed with the follow components and parameters: a Wall-Jet cell (Au, Pd) for

Table 1
Mean concentrations of PAHs and anhydrosugars (ng m^{-3}), as well as average values of $PM_{2.5}$, OC, EC, and K^+ (μg m^{-3}).

	MW	LOD	TEF	La Rábida					Puente Mayorga				
				Annual	Winter	Spring	Summer	Autumn	Annual	Winter	Spring	Summer	Autumn
Phenanthrene	178	0.02	0.001	0.019	0.017	0.041	0.018	0.011	0.047	0.049	0.010	0.056	0.052
Anthracene	178	0.02	0.010	0.000	0.000	0.000	0.000	0.000	0.000	0.000	0.000	0.000	0.000
Fluoranthene	202	0.02	0.001	0.024	0.030	0.015	0.027	0.015	0.042	0.036	0.012	0.066	0.038
Pyrene	202	0.02	0.001	0.023	0.025	0.008	0.029	0.016	0.037	0.032	0.010	0.059	0.034
Benzo(a)anthracene	228	0.02	0.100	0.010	0.011	0.006	0.011	0.009	0.006	0.008	0.003	0.007	0.005
Chrysene	228	0.02	0.010	0.032	0.052	0.012	0.024	0.029	0.041	0.060	0.018	0.036	0.038
Benzo(b)fluoranthene	252	0.02	0.100	0.065	0.101	0.013	0.061	0.053	0.057	0.080	0.021	0.066	0.041
Benzo(k)fluoranthene	252	0.02	0.100	0.017	0.028	0.006	0.012	0.015	0.015	0.023	0.009	0.013	0.012
Benzo(a)pyrene	252	0.03	1.000	0.024	0.033	0.017	0.023	0.016	0.013	0.016	0.010	0.015	0.011
Benzo(ghi)perylene	276	0.03	0.100	0.037	0.046	0.011	0.039	0.035	0.028	0.038	0.012	0.032	0.021
Indeno(123-cd)pyrene	276	0.03	1.000	0.035	0.056	0.010	0.026	0.039	0.035	0.053	0.018	0.022	0.038
Dibenz(a.h)anthracene	278	0.04	0.010	0.000	0.000	0.000	0.000	0.000	0.000	0.000	0.000	0.000	0.000
ΣPAHs	–	–	–	0.284	0.401	0.139	0.271	0.238	0.321	0.395	0.122	0.371	0.291
BaP_{eq}	–	–	–	0.072	0.108	0.031	0.062	0.066	0.059	0.085	0.033	0.049	0.057
Levoglucosan	–	–	–	14.98	37.80	4.85	6.64	10.63	9.78	20.41	6.90	4.44	7.37
Manosan	–	–	–	5.41	15.05	0.43	1.68	4.48	3.07	6.52	1.71	0.99	3.06
Galactosan	–	–	–	2.12	3.57	2.38	1.28	1.25	2.07	2.23	4.16	0.55	1.34
ΣAnhydrosugars	–	–	–	22.51	56.42	7.67	9.58	16.37	14.09	29.16	9.44	5.98	11.78
$PM_{2.5}$	–	–	–	12.92	15.39	10.51	13.31	10.37	14.06	13.58	12.52	15.84	13.55
OC	–	–	–	1.43	1.57	1.13	1.36	1.53	1.29	1.40	0.83	1.28	1.45
EC	–	–	–	0.18	0.21	0.09	0.17	0.22	0.22	0.19	0.12	0.25	0.28
K^+	–	–	–	0.10	0.13	0.06	0.08	0.11	0.08	0.13	0.02	0.06	0.07
Temperature (°C)	–	–	–	18.2	12.4	18.9	24.9	16.5	18.3	14.0	18.1	23.7	17.3

Notes: Molecular weight (MW); Limit of detection (LOD); Toxic equivalency factor (TEF; Nisbet and LaGoy, 1992).

anion analysis of analytes with a gold (3 mm) as working electrode and a palladium reference electrode, spacer of 50 μm, measuring potential 50 mV, measuring range 200 μA, measuring time 100 ms, cycle duration 550 ms and temperature of 32 °C.

2.3. Statistical data analyses

Basic and multivariate statistical analyses, namely Pearson correlations (*r*) and Principal component analysis (PCA), were used for analyzing chemical and meteorological data. For these analyses the STATISTICA version 8 (2008) software package (StatSoft) was used.

PCA was performed with a Varimax rotation of the data matrix, and the principal components (PCs) or factors were extracted in accordance with a series of quality criteria: the number of eigenvalues higher than 1 (Kaiser criterion), the over 10% of total variance and the over 70–85% percentage of cumulative variance explained by the corresponding PCs (Jolliffe and Cadima, 2016). PCA reduces the large number of variables to a few PCs, and this multivariate technique makes it possible to simplify the interpretation for complex systems such as those related to the chemical composition of fine airborne particles. As concerns SLR, Pearson correlation coefficients (r) were checked for the probability (p). When the corresponding "p" values were greater than 0.05, a two-tailed *t*-test was applied with the 95% confidence interval. If the null hypothesis is "$r = 0$", then the two-tailed tests assess whether "r" is significantly different from zero.

2.4. Meteorology and air masses origin

Meteorological data on sampling period were obtained from two stations of the Spanish State Meteorological Agency (AEMET, 2020) located in Moguer (province of Huelva) and Tarifa (province of Cádiz). The coast of Huelva and Cádiz has both temperate Mediterranean and

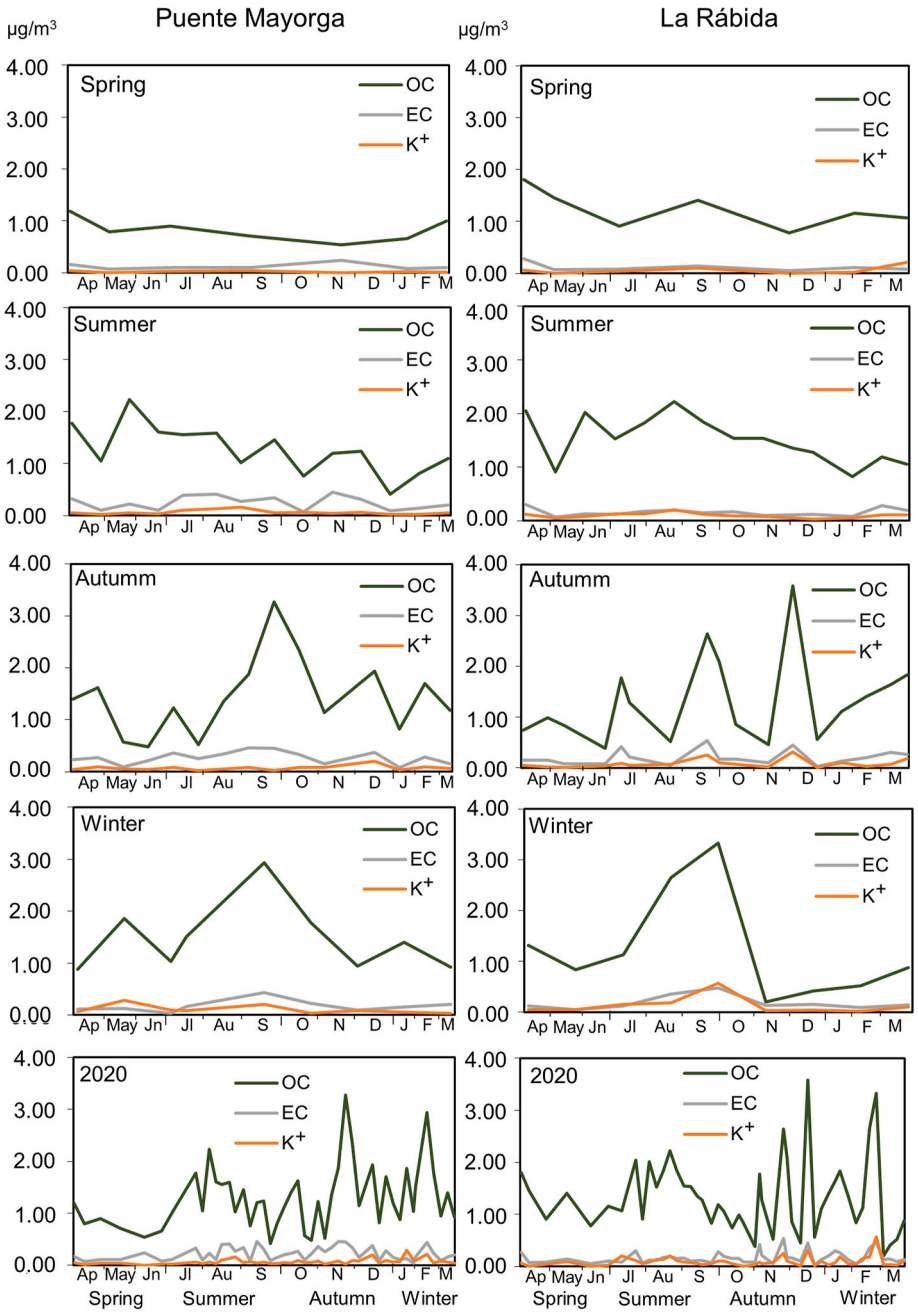

Fig. 2. Seasonal and monthly variation of OC, EC and K^+ in $PM_{2.5}$ for the sampling period at Puente Mayorga and La Rábida.

Atlantic climates (Millán-Martínez et al., 2021). Precipitations are moderate (around 500 and 300 L m^{-2} in 2020, respectively) and occur principally in spring and autumn since winters and summers are dry or very dry at two sampling sites. Average seasonal ambient temperatures near the sampling sites during the period of study are also shown in Table 1. Persistent wind conditions with hardly any change over 24 h in the Bay of Algeciras are dominated by two components, namely easterly (E–SSE) and westerly (W–NNW) winds. One out of every three days was characterized by mixed hourly east and west wind directions (Pandolfi et al., 2011). Two main hourly wind patterns were also identified at the Estuary of Huelva (Millán-Martínez et al., 2021): one due to Atlantic breeze (SW) and the other due to the topographical features of the area (NW–NE). It is also worth noting the more frequent air stagnation conditions in the summer and winter seasons coinciding with irregularity and low rate of precipitation rainfall (de la Rosa et al., 2010).

3. Results and discussion

3.1. $PM_{2.5}$-bound PAH and anhydrosugar levels and seasonal variations

Average levels of the PAHs and anhydrosugars obtained in the current study are shown in Table 1, arranged by sampling site and seasons of the year. Annual and seasonal (winter, spring, summer, and autumn) average concentrations of $PM_{2.5}$, elemental carbon (EC), carbonaceous species or organic carbon (OC), and potassium ion for the Puente Mayorga and La Rábida sampling sites are also shown in Table 1. The $PM_{2.5}$, OC and EC levels were similar in La Rábida and Puente Mayorga, with average annual OC values of 1.43 and 1.29 μg·m^{-3}, EC concentrations of 0.18 and 0.22 μg·m^{-3} on average annually, and $PM_{2.5}$ levels averaging 12.92 and 14.06 μg·m^{-3} over the sampling period, respectively. Fig. 2 shows the time variations of $PM_{2.5}$, EC, OC, and potassium ion (K^+), the latter being a typical biomass burning tracer used in previous studies (Cheng et al., 2013), of fine particles at the two sampling sites.

Fig. 3 shows the ΣPAH concentrations at the two sampling sites in each season. Appreciable seasonal variations were observed for individual compound and the sum of the PAHs at both sites (Table 1 and Fig. 3), with the highest seasonal concentrations registered during winter (post-lockdown period) from December 2020 to February 2021 (averaging c. a. 0.400 ng·m^{-3} in La Rábida and Puente Mayorga) and summer (relaxation period) season (0.271 and 0.371 ng·m^{-3} on average, respectively), coincident with some intervals of highly stable atmospheric conditions that prevent the spread of contaminants and the presence of stationary high pressure systems over southern Spain (e.g., van Drooge and Grimalt, 2015). Attending to meteorological data, certain factors might explain these relatively high levels. Puente Mayorga and La Rábida stations are located in warm Spanish areas (both having annual mean temperatures around 18 °C) with low rainfall (monthly maximum values of 173 and 99 mm in Puente Mayorga and La Rábida, respectively), which favours the resuspension and photodegradation (AEMET, 2020). By contrast, the lowest ΣPAH levels averaging 0.111 and 0.211 ng·m^{-3} in La Rábida and Puente Mayorga during temperate months from mid-March 2020 to early June 2020 (0.284 and 0.321 ng·m^{-3}, respectively, on average annually), coinciding with the lockdown period in Spain. Additional factors might contribute to seasonal variations in PAH concentrations: reduced atmospheric dispersion resulting from lower mixing height, diminished photochemical degradation, and lower atmospheric temperature lead to higher PAH levels in $PM_{2.5}$ samples during winter (Li et al., 2009). Regarding anthropic factors, higher PAH emissions from primary sources of combustion such vehicle exhausts and domestic heating contribute to elevated PAH levels in winter (Ludykar et al., 1999).

BaP is of greatest interest due to its high carcinogenic potency (Huang et al., 2013) and is the only PAH compound in particulate matter

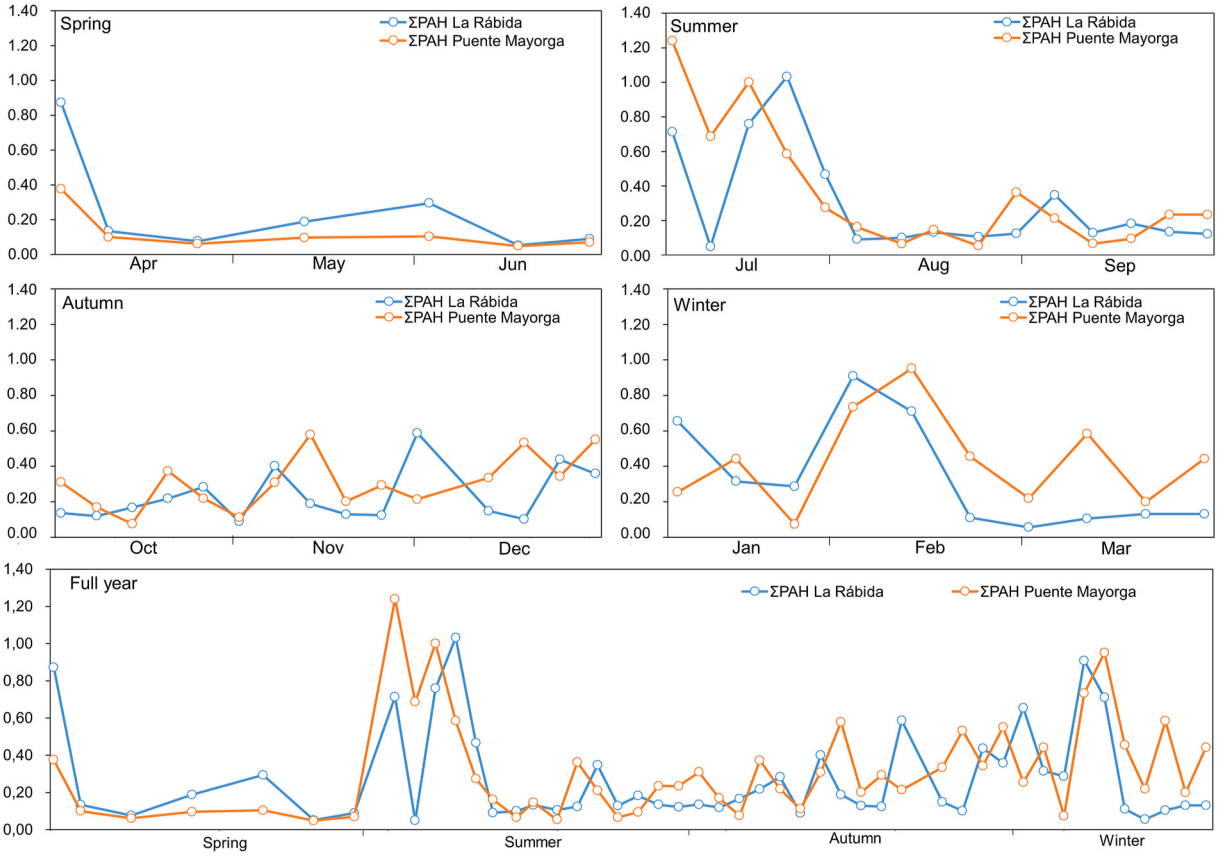

Fig. 3. Seasonal and monthly variation of $PM_{2.5}$, ΣPAHs and Σanhydrosugars for the sampling period at Puente Mayorga and La Rábida.

that is regulated by normative (Directive, 2004/107/EC). The detected BaP annual average concentrations reached 0.024 and 0.013 ng·m^{-3} in La Rábida and Puente Mayorga, respectively, while the maximum concentrations of $PM_{2.5}$-bound BaP were low (around 0.060 ng·m^{-3}) in the areas surrounding the Gibraltar-San Roque and La Rábida refineries.

Results from Estuary of Huelva and Bay of Algeciras point to PAHs with molecular weights (MWs) $\leq$ 202 accounted for 23–30% of ΣPAHs in the fine particle-phase. Most PAHs with MWs > 202 have high relative toxicities (Nisbet and Lagoy, 1992). Except phenanthrene in Estuary of Huelva, measured EPA priority PAHs in both sampling sites reached their minimum concentrations during spring due to the road traffic and industrial activity reduction as a result of the Covid-19 lockdown. Anomalous high phenanthrene levels in La Rábida during the spring season might be explained by the great proximity of the monitoring station to the Huelva Port, where harbour activities continued through the confinement period (Donateo et al., 2014). Chrysene is mainly emitted from industrial oil burning and diesel/gasoline vehicle exhausts; while BghiP is only indicative of gasoline automobile emission (Kulkarni and Venkataraman, 2000; Ho et al., 2002) and BbF or Phe are indicators of biomass burning (Kakareka et al., 2005).

Although the presence of the biomass burning tracer levoglucosan was detected all year in La Rábida and Puente Mayorga because of several causes such as agricultural fires after harvesting (Table 1), the highest levels of Lev and M in winter are suggestive of a higher domestic biomass burning activity during the cold season at both sampling sites (Zhang et al., 2008). Seasonal variations in levels of levoglucosan have also been previously reported (Jedynska et al., 2014). In both sampling sites, samples exhibited values typical for zones with low influence of biomass burning (Puxbaum et al., 2007), with annual maximum concentrations of levoglucosan in $PM_{2.5}$ samples during winter below 50 and 120 ng·m^{-3} near the Gibraltar-San Roque and La Rábida refineries (9.78 and 14.98 ng·m^{-3}, respectively, on average annually). Fig. 3 also shows the sum of the three monosaccharide anhydride concentrations at both sampling sites in each season. The highest Σanhydrosugar levels registered from late November 2020 to mid-January 2021 (averaging 31.73 and 19.29 ng m^{-3} in La Rábida and Puente Mayorga, respectively; see Table 1). This period coincides with the same PAHs variations and with the use of domestic heating systems during the winter season in Southern Spain, such as biomass burning chimneys or pellet stoves (Ren et al., 2022). By contrast, the lowest Σanhydrosugar levels averaging 3.92 and 3.88 ng m^{-3}, respectively, in La Rábida and Puente Mayorga (22.51 and 14.09 ng m^{-3}, respectively, on average annually) from May 2020 to late September 2020, during the warm season.

3.2. Toxicities of $PM_{2.5}$-bound PAHs

Assessing health risk on the basis of the EPA priority PAHs should be investigated. This can be done through toxic equivalent factors (TEFs) for individual PAH compounds using BaP as a reference component (Jung et al., 2010). Thus, the concentration of each PAH compound can be assessed by multiplying its concentration by the respective TEF in order to obtain BaP_{eq} values (see Table 1). As expected from BaP and ΣPAH concentrations, BaP_{eq} were the highest in winter (see Table 1), which is mainly attributed to higher anthropic contributions (Pindado et al., 2009). The seasonal average $PM_{2.5}$-bound BaP_{eq} values (ng·m^{-3}) at both monitoring stations have the trends of winter > autumn ~ summer > spring during the sampling period (Table 1) and winter (c.a. 0.10) > autumn ~ spring (c.a. 0.06) > summer (c.a. 0.04) for the 2018–2019 biennium (unpublished results), respectively. These different trends can be explained by COVID-19 pandemic restrictions affecting Spain in spring 2020, as previously suggested.

The $PM_{2.5}$-bound PAH results obtained from Puente Mayorga and La Rábida are comparable to those reported by Oliveira et al. (2007) in several non-urban sites of Europa, but with significant anthropic contributions due to road traffic and marine transport. Particularly, warm season data were comparable to those obtained at other European rural and industrial areas (ΣPAHs around 1.0 ng·m^{-3}; Pindado et al., 2009). Assuming that PAHs are emitted in large quantities during biomass burning (Alier et al., 2013) and taking into account that BaP_{eq} did not increase notably in winter when compared to annual average values (see Table 1), it could be stated that biomass burning was not the main source of PAHs in the study areas.

3.3. Diagnostic ratios and source appointment

The OC/EC ratios in La Rábida and Puente Mayorga stations averaged annually 8.25 and 6.07, respectively (Table 2). OC/EC ratios ranging from 1.9 to 2.3 in Spain suggest the direct influence of combustion engine emissions, specially diesel motorized vehicle exhausts (Querol et al., 2013); while higher OC/EC ratios probably reflected additional OC sources such as contributions of secondary organic aerosols (SOA) and wood combustion (van Drooge et al., 2022). Biomass burning emissions make important contributions to OC and PAHs, but they are lower contributors to EC compared to road traffic and maritime transport emissions (Schauer et al., 2008).

Table 2 also shows information on several PAH isomeric diagnostic ratios. These parameters have been used to identify sources of combustion, even though there are not definitive values for a given source (Tobiszewski and Namiesnik, 2012). Undetectable levels of Anth compared to Phen in both sampling sites suggest photodegradation of low molecular weight PAHs (Ladji et al., 2007) and are probably due to the lower photolability of the latter (Wild et al., 2005). Negligible concentrations of BeP in relation to BaP in aerosols may indicate fresh combustion emissions when compared to aged aerosols due to photochemical degradation (Galarneau, 2008). Mean annual Flt/(Pyr + Flt), Ind/(BghiP + Ind), BaA/BaP, and BaA/(Chry + BaA) ratios of around 0.5, >0.5, <0.5, and <0.3 for both stations would be indicative of a variety of sources (traffic, industry, and others) of $PM_{2.5}$-bound PAHs in La Rábida and Puente Mayorga.

The monosaccharide anhydride levoglucosan has been used to determine the relative contribution of biomass burning through the ratio Lev/OC in wood burning smoke emissions (Maenhout et al., 2012). This ratio averaged annually 0.012 and 0.009, respectively, in La Rábida and Puente Mayorga (Table 2), showing lower contributions of biomass burning in the latter sampling station. As expected, Lev/OC averages increased to 0.027 and 0.015 during winter, respectively, in La Rábida and Puente Mayorga. These levels are comparable with most of observations at urban sites (e.g., Cheng et al., 2013). However, Lev/OC values decreased in both sampling sites during the warm season in this study (Table 2), suggesting that the contribution from biomass burning was thereby diminished. In addition, Lev/K^+ averaged 0.29 and 0.20 during winter, respectively, in La Rábida and Puente Mayorga. These mean values were lower than those (c.a. 0.50) during winter time at urban sites (e.g., Cheng et al., 2013). Annually, Lev/K^+ mean values decreased to 0.14 and 0.13, respectively, in La Rábida and Puente Mayorga (Table 2), indicating a minor contribution from biomass burning during the other seasons (Chantara et al., 2019).

Levoglucosan and mannosan were correlated well (r > 0.9) during the sampling period in both sites. The Lev/M ratio in smoke plumes from hardwood and softwood burning have been characterized by values in the ranges of 11–146 (28 on average) and 2.5 to 4.7 (4.3 on average), respectively (Jung et al., 2014). The Lev/M values in La Rábida and Puente Mayorga, averaging annually 3.30 and 3.52 in $PM_{2.5}$ (Table 2), respectively, may indicate a limited influence of hardwood combustion in the two areas of study. More precisely, the highest Lev/M ratios in Puente Mayorga were observed on July and September during several one-day episodes, with peak values from 18.42 to 38.02 notably higher than the seasonal average (4.45), which might be explained by the fact that crop residue and/or other burning aerosols can be transported long distances downwind from the source areas (e.g., Liang et al., 2020; Cheng et al., 2022). These episodes did not occur in August 2020, which is the typical month for holidays, suggesting that they may be partially

Table 2
OC/EC, PAH and other diagnostic ratios.

Ratio	La Rábida					Puente Mayorga				
	Annual	Spring	Summer	Autumn	Winter	Annual	Spring	Summer	Autumn	Winter
OC/EC	8.25	10.37	9.23	6.50	6.90	6.07	6.66	5.24	5.27	7.13
Lev/OC	0.012	0.006	0.004	0.012	0.027	0.009	0.013	0.003	0.005	0.015
Lev/M	3.30	5.26	2.36	3.07	2.51	3.52	3.95	4.45	2.54	3.13
Lev/K^+	0.14	0.11	0.04	0.15	0.29	0.13	0.15	0.07	0.10	0.20
Ind/(BghiP + Ind)	0.51	0.54	0.40	0.53	0.58	0.56	0.59	0.44	0.63	0.58
BaA/BaP	0.42	0.26	0.43	0.63	0.36	0.43	0.30	0.44	0.46	0.54
Flt/(Pyr + Flt)	0.50	0.57	0.47	0.48	0.51	0.51	0.53	0.49	0.52	0.51
BaA/(Chry + BaA)	0.26	0.35	0.33	0.25	0.12	0.13	0.14	0.15	0.12	0.12

caused in this case by grass burning after brush clearing (Sullivan et al., 2008). This brush clearing activity is usual in Andalusia during the early spring in order to reduce the risk of forest fires in summer, however, the COVID-19 pandemic delayed it until the summer 2020 in some Andalusian areas. By contrast, in spring, the peak values of Lev/M in La Rábida (13.40–35.06) were higher than those in Puente Mayorga (5.86–9.90). The lowest Lev/M averages were found in the cold seasons (Table 2), with values ranging from 0.62 to 3.67 in La Rábida and from 0.87 to 5.18 in Puente Mayorga.

3.4. Relationship among PAHs, OC and other air pollutants

Correlations between the $PM_{2.5}$-bound ΣPAH concentrations and other air contaminants in $PM_{2.5}$ have been used to elucidate the emission sources for these compounds in the ambient air (Crimmins et al., 2004). Our findings indicate that such correlations were appreciably different among seasons (Table 3). In autumn and winter (post-lockdown period), ΣPAHs showed good relationship with EC and OC of fine particles, with positive Pearson correlation coefficients (r) exceeding 0.4. In summer (Relaxation and post-lockdown periods) it is noteworthy to mention that ΣPAHs showed a significant correlation with OC (>0.4) instead of EC (<0.1). This might reveal that PAHs and OC, unlike EC, were generated from the same sources in this season. In spring (lockdown period), fine particle PAHs were negatively or not correlated with OC and EC, respectively, in Puente Mayorga and La Rábida. In all seasons, the correlation coefficients between ΣPAHs and EC are lower than those between ΣPAHs and OC, which could be might be explained by the influence of gasoline automobile emissions (Kim et al., 2012) and by the fact that EC is less abundant than OC in smoke plumes from biomass burning (Pósfai et al., 2003). The relationship between PAHs and K^+ showed similar seasonal variation than that between OC and K^+ in La Rábida, while PAHs showed no or inverse relationship with potassium ion in Puente Mayorga in all seasons (Table 3).

Finally, despite the fact that $PM_{2.5}$-bound ΣPAH and OC levels are often negatively correlated to the ambient temperature because of the semi-volative character of these compounds (Li et al., 2009), little correlations were observed between both levels and temperature throughout the year in Estuary of Huelva and Bay of Algeciras probably due to more stable atmospheric conditions favouring resuspension of soil dust and photochemical activity in warm seasons.

3.5. Principal component analysis (PCA)

The differences among data were studied using PCA. This was done in order to determine the sources of PAHs and anhydrosugars in $PM_{2.5}$. The results from the Sequential Principal Component Analysis of OC, EC, K^+, PAHs and monosaccharide anhydrides were obtained for all samples collected during the 2020–2021 annual period in both stations. A Pearson correlation study and a PCA performed until 95% of the total variance allowed us to find the following groups of interrelated variables: a) levoglucosan and mannosan with Ind, Chry and BkF; b) BghiP, BbF and BaP with Lev and Man. After removal of variables with low communalities (non-significant), the four PCs accounted for 79.3% of the total variance (Table 4).

PC1 accounted for 41.2% of the total variance and appeared grouping of the less volatile PAHs: BghiP, BbF, BaP, BaA, BkF, Ind and Chry with high positive loadings (0.70–0.94). The higher scores were found in samples collected during two periods: first, those collected during weekends in June and July 2020, probably due to people commuting into the study areas throughout the summer, and second, samples collected on weekdays in January 2021 and the Christmas day date in 2020. Therefore, this group of high concentrations of heavy

Table 3
Pearson correlation coefficients (r) among OC, EC, K^+ and ΣPAHs.

	La Rábida						Puente Mayorga				
		OC	EC	K^+	PAHs			OC	EC	K^+	PAHs
Spring	OC	1	–	–	–	Spring	OC	1	–	–	–
	EC	0.617	1	–	–		EC	(0.135)	1	–	–
	K^+	0.028	0.091	1	–		K^+	0.597	(0.191)	1	–
	PAHs	(0.227)	(0.242)	(0.280)	1		PAHs	0.044	0.024	0.098	1
Summer	OC	1	–	–	–	Summer	OC	1	–	–	–
	EC	0.469	1	–	–		EC	0.460	1	–	–
	K^+	0.701	0.484	1	–		K^+	0.168	0.468	1	–
	PAHs	0.465	0.124	0.208	1		PAHs	0.413	0.040	(0.240)	1
Autumn	OC	1	–	–	–	Autumn	OC	1	–	–	–
	EC	0.865	1	–	–		EC	0.728	1	–	–
	K^+	0.898	0.795	1	–		K^+	0.245	0.272	1	–
	PAHs	0.766	0.693	0.703	1		PAHs	0.662	0.442	0.094	1
Winter	OC	1	–	–	–	Winter	OC	1	–	–	–
	EC	0.913	1	–	–		EC	0.584	1	–	–
	K^+	0.873	0.889	1	–		K^+	0.571	0.084	1	–
	PAHs	0.631	0.556	0.449	1		PAHs	0.760	0.460	0.097	1

Note: negative values in parenthesis.

Table 4
Eigenvalues, variances (%) and PCA variable loadings of four principal components.

	PC1	PC2	PC3	PC4
Phe	(0.03)	(0.05)	0.88	0.04
Flt	0.39	(0.06)	0.86	(0.04)
Pyr	0.52	(0.09)	0.78	0.01
BaA	0.89	(0.05)	0.13	0.01
Chry	0.70	0.27	0.22	0.38
BbF	0.93	0.12	0.20	0.16
BkF	0.86	0.25	0.10	0.29
BaP	0.90	0.06	0.07	0.08
BghiP	0.94	0.07	0.21	0.15
Ind	0.76	0.24	0.05	0.43
G	0.18	0.62	(0.16)	0.36
M	0.32	0.71	(0.04)	0.42
Lev	0.40	0.79	(0.05)	0.36
OC	0.51	(0.03)	(0.05)	0.70
EC	0.18	(0.13)	0.12	0.81
K	0.32	0.06	(0.20)	0.71
Eigenvalues	8.2	4.2	2.3	1.2
Total variance	41.2	20.9	11.3	5.9
Cumulative variance	41.2	62.1	73.4	79.3

Note: negative values in parenthesis.

PAHs is associated to combustion engine vehicle emissions even in these two industrial areas.

PC2 explained 20.9% of the total variance, and it is characterized by the concentrations of Lev, M and G, with high positive loadings (0.62–0.79), indicating high emissions of anhydrosugars on cold days, particularly in winter. This second principal component is related with the results of the cold season as commented above. Based on the representative scores, the samples associated in both sampling stations were collected from late November 2020 to mid-January 2021, showing the highest coefficients for fine particles collected on really cold days at the end of 2020 and beginning of 2021. Therefore, this grouping of high concentrations of Lev, M and G can be associated to biomass burning of wood in chimneys and pellets' stoves at home (Cheng et al., 2013).

PC3 accounted for 11.3% of the total variance and grouped the light PAHs: Flt, Pyr and Phe (positive loadings of 0.78–0.86) associated mainly to Puente Mayorga and some samples from La Rábida. In this research work, Phe, Flt and Pyr can be associated with ship emissions in coastal areas near important harbours (Valavanidis et al., 2006), such as the two complex industrial zones under study. Regarding representative samples of PC3, 44% of high scores correspond to $PM_{2.5}$ collected in summer and 28% in all holiday weekends from 9 October to December 20, 2020. Therefore, in this case PC3 was attributed to PAHs emitted from domestic wood burning and wood-based waste combustion (Kakareka et al., 2005; Park et al., 2013). Finally, PC4 explained 5.9% of the total variance and is characterized by the levels of OC, EC and K^+ (positive loadings of 0.70–0.81) and to a lesser content anhydrosugars. The highest scores were found in samples from both industrial zones collected in March–July and September 2020, but not in August, suggesting that grass burning under anticyclonic conditions as previously mentioned.

4. Conclusions

Limiting human mobility imposed by the Spanish Government across the country during part of the year 2020 by the coronavirus disease 2019 (Covid-19) brought about exceptional conditions for investigating the evolution of air organic contaminant concentrations. In this work, seasonal PAH and monosaccharide anhydride concentrations in $PM_{2.5}$ fraction were studied from March 2020 to March 2021 in Puente Mayorga and La Rábida (Southern Spain). Results indicated a decrease in $PM_{2.5}$-bound ΣPAH concentrations in the study areas during the confinement period resulting from diminution of road traffic emissions.

In Bay of Algeciras and Estuary of Huelva, the highest seasonal ΣPAH concentrations in 2020 were recorded during winter (post-lockdown period) and summer (relaxation and post-lockdown periods), coincident with climate factors such as low rainfall, dry soils favouring resuspension and/or high photodegradation in the two study areas. In both cases, levels of anhydrosugars, diagnostic ratios and multivariate analysis suggest contributions from the road traffic emissions, shipping oil combustion and industrial estate, along with a definite influence of biomass burning.

Credit author statement

M.A. Guzmán: Investigation, Formal Analysis, Writing - Original Draft. **A.J. Fernández**: Writing - Original Draft, Software, Formal Analysis. **C. Boente**: Data Curation, Investigation, Formal Analysis, Visualization. **G. Márquez**: Methodology, Resources, Writing – Original Draft, Data Acquisition, Supervision, Validation. **A. Sánchez de la Campa**: Writing - Review & Editing, Resources. **E. Lorenzo**: Data Curation, Investigation, Visualization.

Declaration of competing interest

The authors declare that they have no known competing financial interests or personal relationships that could have appeared to influence the work reported in this paper.

Acknowledgments

We are grateful to the project of the Ministry of Science, Innovation and Universities of Spain (Project RTI 2018-095937-B-I00), the co-financed project by the Andalusian Government and the EU (PY18-2332), and the Environmental Agency of Andalusia for financial and technical support. Carlos Boente obtained a post-doctoral contract within the program PAIDI 2020 (Ref 707 DOC 01097), co-financed by the Junta de Andalucía (Spain) and the EU. Funding for open access charge: Universidad de Huelva / CBUA.

References

AEMET, 2020. https://opendata.aemet.es/centrodedescargas/productosAEMET.

Alam, M.S., Keyte, I.J., Yin, J., Stark, C., Jones, A.M., Harrison, R.M., 2015. Diurnal variability of polycyclic aromatic compound (PAC) concentrations: relationship with meteorological conditions and inferred sources. Atmos. Environ. 122, 427–438. https://doi.org/10.1016/j.atmosenv.2015.09.050.

Alier, M., van Drooge, B.L., Dall'Osto, M., Querol, X., Grimalt, J.O., Tauler, R., 2013. Source apportionment of submicron organic aerosol at an urban background and a road site in Barcelona (Spain) during SAPUSS. Atmos. Chem. Phys. 13, 10353–10371. https://doi.org/10.5194/acp-13-10353-2013.

Amato, F., Alastuey, A., Karanasiou, A., Lucarelli, F., Nava, S., Calzolai, G., Severi, M., Becagli, S., Gianelle, V.L., Colombi, C., Alves, C., Custodio, D., Nunes, T., Cerqueira, M., Pio, C., Eleftheriadis, K., Diapouli, E., Reche, C., Minguillon, M.C., Manousakas, M.-I., Maggos, T., Vratolis, S., Harrison, R.M., Querol, X., 2016. AIRUSE-LIFE+: a harmonized PM speciation and source apportionment in five southern European cities. Atmos. Chem. Phys. 16, 3289–3309. https://doi.org/10.5194/acp-16-3289-2016.

Chantara, S., Thepnuan, D., Wiriya, W., Prawan, S., Tsai, Y.I., 2019. Emissions of pollutant gases, fine particulate matters and their significant tracers from biomass burning in an open-system combustion chamber. Chemosphere 224, 407–416. https://doi.org/10.1016/j.chemosphere.2019.02.153.

Chen, Y.-C., Chiang, H.-C., Hsu, C.-Y., Yang, T.-T., Lin, T.-Y., Chen, M.-J., Chen, N.-T., Wu, Y.-C., 2016. Ambient $PM_{2.5}$-bound polycyclic aromatic hydrocarbons (PAHs) in Changhua County, central Taiwan: seasonal variation, source apportionment and cancer risk assessment. Environ. Pollut. 218, 372–382. https://doi.org/10.1016/j.envpol.2016.07.016.

Cheng, Y., Cao, X., Liu, J., Yu, Q., Zhong, Y., Geng, G., Zhang, Q., He, K., 2022. New open burning policy reshaped the aerosol characteristics of agricultural fire episodes in Northeast China. Sci. Total Environ. 810, 152272 https://doi.org/10.1016/j.scitotenv.2021.152272.

Cheng, Y., Engling, G., He, K.B., Duan, F.K., Ma, Y.L., Du, Z.Y., Liu, J.M., Zheng, M., Weber, R.J., 2013. Biomass burning contribution to Beijing aerosol. Atmos. Chem. Phys. 13, 7765–7781. https://doi.org/10.5194/acp-13-7765-2013.

Choi, S.D., Baek, S.Y., Chang, Y.S., 2007. Influence of a large steel complex on the spatial distribution of volatile polycyclic aromatic hydrocarbons (PAHs) determined by passive air sampling using membrane-enclosed copolymer (MECOP). Atmos. Environ. 41, 6255–6264. https://doi.org/10.1016/j.atmosenv.2007.03.058.

Crimmins, B.S., Dickerson, R.R., Doddridge, B.G., Baker, J.E., 2004. Particulate polycyclic aromatic hydrocarbons in the Atlantic and Indian Ocean atmospheres during the Indian Ocean experiment and aerosols: continental sources to the marine atmosphere. J. Geophys. Res. Atmos. 109, D05308 https://doi.org/10.1029/2003JD004192.

De la Rosa, J.D., Sánchez de la Campa, A.M., Alastuey, A., Querol, X., González-Castanedo, Y., Fernández-Camacho, R., Stein, A.F., 2010. Using PM10 geochemical maps for defining the origin of atmospheric pollution in Andalusia (Southern Spain). Atmos. Environ. 44, 4595–4605. https://doi.org/10.1016/j.atmosenv.2010.08.009.

Donateo, A., Gregoris, E., Gambaro, A., Merico, E., Giua, R., Nocioni, A., Contini, D., 2014. Contribution of harbour activities and ship traffic to PM2.5, particle number concentrations and PAHs in a port city of the Mediterranean Sea (Italy). Environ. Sci. Pollut. Res. 21, 9415–9429. https://doi.org/10.1007/s11356-014-2849-0.

European Commission, 2015. Commission regulation 2015/1189 implementing Directive 2009/125/EC of the European Parliament and of the Council with regard to ecodesign requirements for solid fuel boilers. https://eur-lex.europa.eu/eli/reg/2015/1189/2017-01-09.

Fontal, M., van Drooge, B.L., López, J.F., Fernández, P., Grimalt, J.O., 2015. Broad spectrum analysis of polar and apolar organic compounds insubmicron atmospheric particles. J. Cromatogr. 1404, 28–38. https://doi.org/10.1016/j.chroma.2015.05.042.

Galarneau, E., 2008. Source specifity and atmospheric processing of airborne PAHs: implications for source apportionment. Atmos. Environ. 42, 8139–8149. https://doi.org/10.1016/j.atmosenv.2008.07.025.

Ho, K.F., Lee, S.C., Chiu, G.M.Y., 2002. Characterization of selected volatile organic compounds, polycyclic aromatic hydrocarbons and carbonyl compounds at a roadside monitoring station. Atmos. Environ. 36, 57–65. https://doi.org/10.1016/S1352-2310(01)00475-7.

Huang, D.-Y., Zhou, S.-G., Hong, W., Feng, W.-F., Tao, L., 2013. Pollution characteristics of volatile organic compounds, polycyclic aromatic hydrocarbons and phthalate esters emitted from plastic wastes recycling granulation plants in Xingtan Town, South China. Atmos. Environ. 71, 327–334. https://doi.org/10.1016/j.atmosenv.2013.02.011.

IARC Working Group, 2010. Benzo[a]pyrene iarc monographs on the identification of carcinogenic hazards to humans. Accessed on 11 January 2023. Available online: https://monographs.iarc.who.int/wp-content/uploads/2018/06/mono100F-14.pdf.

Jedynska, A., Hoek, G., Wang, M., Eefteno, M., Cyrys, J., Beelen, R., Cirach, M., Denazelle, A., Nystad, W., Makaem Akhlaghi, H., Meliefste, K., Nieuwenhuijsen, M., de Hoogh, K., Brunefreef, B., Kooter, I.M., 2014. Spatial variations and development of land use regression models of levoglucosan in four European study areas. Atmos. Chem. Phys. Discuss. 14, 13491–13572. https://doi.org/10.5194/acpd-14-13491-2014.

Jolliffe, I.T., Cadima, J., 2016. Principal component analysis: a review and recent developments. Phil. Trans. R. Soc. A 374, 20150202. https://doi.org/10.1098/rsta.2015.0202.

Jung, J., Lee, S., Kim, H., Kim, D., Lee, H., Oh, S., 2014. Quantitative determination of the biomass-burning contribution to atmospheric carbonaceous aerosols in Daejeon, Korea, during the rice-harvest period. Atmos. Environ. 89, 642–650. https://doi.org/10.1016/j.atmosenv.2014.03.010.

Jung, K.H., Yan, B., Chillrud, S.N., Perera, F.P., Whyatt, R., Camann, D., Kinney, P.L., Miller, R.L., 2010. Assessment of Benzo(a)pyrene-equivalent carcinogenicity and mutagenicity of residential indoor versus outdoor polycyclic aromatic hydrocarbons exposing young children in New York City. Int. J. Environ. Res. Publ. Health 7, 1889–1900. https://doi.org/10.3390/ijerph7051889.

Kakareka, S.V., Kukharchyk, T.I., Khomich, V.S., 2005. Study of PAH emission from the solid fuels combustion in residential furnaces. Environ. Pol. 133, 383–387. https://doi.org/10.1016/j.envpol.2004.01.009.

Kappos, A.D., Bruckmann, P., Eikmann, T., Englert, N., Heinrich, U., Hoppe, P., Koch, E., Krause, G.H.M., Kreyling, W.G., Rauchfuss, K., Rombout, P., Schulz-Klemp, V., Thiel, W.R., Wichmann, H.E., 2004. Health effects of particles in ambient air. Int. J. Hyg Environ. Health 207, 399–407. https://doi.org/10.1078/1438-4639-00306.

Kim, J.Y., Lee, J.Y., Choi, S.-D., Kim, Y.P., Ghim, Y.S., 2012. Gaseous and particulate polycyclic aromatic hydrocarbons at the Gosan background site in East Asia. Atmos. Environ. 49, 311–319. https://doi.org/10.1016/j.atmosenv.2011.11.029.

Kulkarni, P., Venkataraman, C., 2000. Atmospheric polycyclic aromatic hydrocarbons in Mumbai, India. Atmos. Environ. 34, 2785–2790. https://doi.org/10.1016/S1352-2310(99)00312-X.

Ladji, R., Yassaa, N., Cecinato, A., Meklati, B.Y., 2007. Seasonal variation of particulate organic compounds in atmospheric PM10 in the biggest municipal waste landfill of Algeria. Atmos. Res. 86, 249–260. https://doi.org/10.1016/j.atmosres.2007.06.002.

Li, Z., Porter, E.N., Sjodin, A., Needham, L.L., Lee, S., Russell, A.G., Mulholland, J.A., 2009. Characterization of PM2.5-bound polycyclic aromatic hydrocarbons in Atlanta—seasonal variations at urban, suburban, and rural ambient air monitoring sites. Atmos. Environ. 43, 4187–4193. https://doi.org/10.1016/j.atmosenv.2009.05.031.

Liang, L., Engling, G., Cheng, Y., Liu, X., Du, Z., Ma, Q., Zhang, X., Sun, J., Xu, W., Liu, C., Zhang 477, G., Xu, H., 2020. Biomass burning impacts on ambient aerosol at a background site in East China: insights from a yearlong study. Atmos. Res. 231, 104660 https://doi.org/10.1016/j.atmosres.2019.104660.

López-Ayala, O., González-Hernández, L.-T., Alcantar-Rosales, V.-M., Elizarragaz-de la Rosa, D., Heras-Ramírez, M.-E., Silva-Vidaurri, L.-G., Alfaro-Barbosa, J.-M., Gaspar-Ramírez, O., 2019. Levels of polycyclic aromatic hydrocarbons associated with particulate matter in a highly urbanized and industrialized region in northeastern Mexico. Atmos. Pollut. Res. 10, 1655–1662. https://doi.org/10.1016/j.apr.2019.06.006.

Ludykar, D., Westerholm, R., Almen, J., 1999. Cold start emissions at +22, -7 and -20 degrees C ambient temperatures from a three-way catalyst (TWC) car: regulated and unregulated exhaust components. Sci. Total Environ. 235, 65–69. https://doi.org/10.1016/j.jes.2017.01.014.

Maenhout, W., Vermeylen, R., Cleays, M., Vercauteren, J., Matheeusesen, C., Roekens, E., 2012. Assessment of the contribution from wood burning to the PM10 aerosol in Flanders, Belgium. Sci. Total Environ. 437, 226–236. https://doi.org/10.1016/j.scitotenv.2012.08.015.

Millán-Martínez, M., Sánchez-Rodas, D., Sánchez de la Campa, A.M., Alastuey, A., Querol, X., de la Rosa, J.D., 2021. Source contribution and origin of PM10 and arsenic in a complex industrial region (Huelva, SW Spain). Environ. Pollut. 274, 116268–116278. https://doi.org/10.1016/j.envpol.2020.116268.

Millán-Martínez, M., Sánchez-Rodas, D., Sánchez de la Campa, A.M., de la Rosa, J., 2022. Impact of the SARS-CoV-2 lockdown measures in Southern Spain on PM10 trace element and gaseous pollutant concentrations. Chemosphere 303, 134853. https://doi.org/10.1016/j.chemosphere.2022.134853.

Nisbet, C., LaGoy, P., 1992. Toxic equivalency factors (TEFs) for polycyclic aromatic hydrocarbons (PAHs). Regul. Toxicol. Pharmacol. 16, 290–300. https://doi.org/10.1016/0273-2300(92)90009-X.

Oliveira, T.S., Pio, C.A., Alves, C.A., Silvestre, A.J.D., Evtyugina, M., Afonso, J.V., Fialho, P., Legrand, M., Puxbaum, H., Gelencsér, A., 2007. Seasonal variation of particulate lipophilic organic compounds at nonurban sites in Europe. J. Geophys. Res. 112, D23S09. https://doi.org/10.1029/2007JD008504.

Pandolfi, M., González-Castanedo, Y., Alastuey, A., de la Rosa, J., Mantilla, E., Sánchez de la Campa, A.M., Querol, X., Pey, J., Amato, F., Moreno, T., 2011. Source apportionment of PM10 and PM2.5 at multiple sites in the strait of Gibraltar by PMF: impact of shipping emissions. Environ. Sci. Pollut. Res. 18, 260–269. https://doi.org/10.1007/s11356-010-0373-4.

Park, S.-S., Sim, S.Y., Bae, M.-S., Schauer, J.J., 2013. Size distribution of water-soluble components in particulate matter emitted from biomass burning. Atmos. Environ. 73, 62–72. https://doi.org/10.1016/j.atmosenv.2013.03.025.

Pérez-Pastor, R., Salvador, P., García-Alonso, S., Alastuey, A., García dos Santos, S., Querol, X., Artiñano, B., 2020. Characterization of organic aerosol at a rural site influenced by olive waste biomass burning. Chemosphere 248, 125896. https://doi.org/10.1016/j.chemosphere.2020.125896.

Pindado, O., Pérez, R., García, S., Sánchez, M., Galán, P., Fernández, M., 2009. Characterization and sources assignment of PM2.5 organic aerosol in a rural area of Spain. Atmos. Environ. 43, 2796–2803. https://doi.org/10.1016/j.atmosenv.2009.02.046.

Pósfai, M., Simonics, R., Li, J., Hobbs, P.V., Buseck, P.R., 2003. Individual aerosol particles from biomass burning in southern Africa: 1. Compositions and size distributions of carbonaceous particles. J. Geophys. Res. Atmos. 108 (D13), 8483. https://doi.org/10.1016/j.atmosenv.2009.02.046.

Puxbaum, H., Caseiro, A., S anchez-Ochoa, A., Kasper-Giebl, A., Cleays, M., Gelencser, A., Legrand, M., Preunkert, S., Pio, C., 2007. Levoglucosan levels at background sites in Europe for assessing the impact of biomass combustion on the European aerosol background. J. Geophys. Res. 112, D23S05. https://doi.org/10.1029/2006JD008114.

Querol, X., Alastuey, A., Viana, M., Moreno, T., Reche, C., Minguillon, M.C., Ripoll, A., Pandolfi, M., Amato, F., Karanasiou, A., Pérez, N., Pey, J., Cusack, M., Vázquez, R., Plana, F., Dall'Osto, M., de la Rosa, J., Sánchez de la Campa, A., Fernández-Camacho, R., Rodríguez, S., Pio, C., Alados-Arboledas, L., Titos, G., Artíñano, B., Salvador, P., García Dos Santos, S., Fernández Patier, R., 2013. Variability of carbonaceous aerosols in remote, rural, urban and industrial environments in Spain: implications for air quality policy. Atmos. Chem. Phys. 13, 6185–6206. https://doi.org/10.5194/acp-13-6185-2013.

Querol, X., Massagué, J., Alastuey, A., Moreno, T., Gangoiti, G., Mantilla, E., Duéguez, J. J., Escudero, M., Monfort, E., Pérez García-Pando, C., Petetin, H., Jorba, O., Vázquez, V., de la Rosa, J., Campos, A., Muñoz, M., Monge, S., Hervás, M., Javato, R., Cornide, M.J., 2021. Lessons from the COVID-19 air pollution decrease in Spain: now what? Sci. Total Environ. 779, 146380 https://doi.org/10.1016/j.scitotenv.2021.146380.

Ravindra, K., Bencs, L., Wauters, E., Hoog, J., Deutsch, F., Roekens, E., Bleux, B., Berghmans, P., Grieken, R.V., 2006. Seasonal and site-specific variation in vapour and aerosol phase PAHs over Flanders (Belgium) and their relation with anthropogenic activities. Atmos. Environ. 40, 771–785. https://doi.org/10.1016/j.atmosenv.2005.10.011.

Ren, Y., Wang, G., Li, H., 2022. Spatial and seasonal variations of primary and secondary organic aerosols at urban areas and continental background site of China: ambient levels, size distribution, and sources. Gondwana Res. 110, 319–329. https://doi.org/10.1016/j.gr.2022.04.005.

Sánchez de la Campa, A.M., Salvador, P., Fernández-Camacho, R., Artíñano, B., Coz, E., Márquez, G., Sánchez-Rodas, D., De la Rosa, J., 2018. Characterization of biomass burning from olive grove areas: a major source of organic aerosol in PM_{10} of Southwest Europe. Atmos. Res. 199, 1–13. https://doi.org/10.1016/j.atmosres.2017.07.032.

Schauer, J.J., Rogge, W.F., Hildemann, L.M., Mazurek, M.A., Cass, G.R., Simoneit, B.R.T., 2007. Source apportionment of airborne particulate matter using organic compounds as tracers. Atmos. Environ. 41, 241–259. https://doi.org/10.1016/1352-2310(96)00085-4.

Sullivan, A.P., Holden, A.S., Patterson, L.A., McMeeking, G.R., Kreidenweis, S.M., Malm, W.C., Hao, W.M., Wold, C.E., Collett Jr., J.L., 2008. A method for smoke marker measurements and its potential application for determining the contribution of biomass burning from wildfires and prescribed fires to ambient $PM_{2.5}$ organic carbon. J. Geophys. Res. 113, D22302 https://doi.org/10.1029/2008JD010216.

Tobiszewski, M., Namiesnik, J., 2012. PAH diagnostic ratios for the identification of pollution emission sources. Environ. Pollut. 162, 110–119. https://doi.org/10.1016/j.envpol.2011.10.025.

Valavanidis, A., Fiotakis, K., Vlahogianni, T., Bakeas, E.B., Triantafillaki, S., Paraskevopoulou, V., Dassenakis, M., 2006. Characterization of atmospheric particulates, particle-bound transition metals and polycyclic aromatic hydrocarbons of urban air in the centre of Athens (Greece). Chemosphere 65, 760–768. https://doi.org/10.1016/j.chemosphere.2006.03.052.

van Drooge, B.L., Grimalt, J.O., 2015. Particle size-resolved source apportionment of primary and secondary organic tracer compounds at urban and rural locations in Spain. Atmos. Chem. Phys. 15, 7735–7752. https://doi.org/10.5194/acp-15-7735-2015.

van Den Heuvel, R., Staelens, J., Koppen, G., Schoeters, G., 2018. Toxicity of Urban PM_{10} and relation with tracers of biomass burning. Int. J. Environ. Res. Publ. Health 15, 320–339. https://doi.org/10.3390/ijerph15020320.

van Drooge, B.L., Garatachea, R., Reche, C., Titos, G., Alastuey, A., Lyamani, H., Alados-Arboledas, L., Querol, X., Grimalt, J.O., 2022. Primary and secondary organic winter aerosols in Mediterranean cities under different mixing layer conditions (Barcelona and Granada). Environ. Sci. Pollut. Res. 29, 36255–36272. https://doi.org/10.1007/s11356-021-16366-0.

Vega, E., López-Veneroni, D., Ramírez, O., Chow, J.C., Watson, J.G., 2021. Particle-bound PAHs and chemical composition, sources and health risk of $PM_{2.5}$ in a highly industrialized area. Aerosol Air Qual. Res. 21, 210047 https://doi.org/10.4209/aaqr.210047.

Vicente, E.D., Alves, C.A., 2018. An overview of particulate emissions from residential biomass combustion. Atmos. Res. 199, 159–185. https://doi.org/10.1016/j.atmosres.2017.08.027.

Wild, E., Dent, J., Thomas, G.O., Jones, K.C., 2005. Real-time visualization and quantification of PAH photodegradation on and within plant leaves. Environ. Sci. Technol. 268–273. https://doi.org/10.1021/es0494196, 2005.

Zhang, T., Claeys, M., Cachier, H., Dong, S.P., Wang, W., Maenhaut, W., Liu, X.D., 2008. Identification and estimation of the biomass burning contribution to Beijing aerosol using levoglucosan as a molecular marker. Atmos. Environ. 42, 7013–7021. https://doi.org/10.1016/j.atmosenv.2008.04.050.